

Size dependence of second-order hyperpolarizability of finite periodic chains under Su-Schrieffer-Heeger model

SHIDONG JIANG¹ and MINZHONG XU²(*)

¹ *Department of Mathematical Sciences, New Jersey Institute of Technology, Newark, NJ 07102*

² *Department of Chemistry, New York University, New York, NY 10003*

PACS. 78.66.Qn – Polymers; organic compounds.

PACS. 42.65.An – Optical susceptibility, hyperpolarizability.

PACS. 78.20.Bh – Theory, models, and numerical simulation.

Abstract. – The second hyperpolarizability $\gamma_N(-3\omega; \omega, \omega, \omega)$ of N double-bond finite chain of trans-polyacetylene is analyzed using the Su-Schrieffer-Heeger model to explain qualitative features of the size-dependence behavior of γ_N . Our study shows that γ_N/N is *nonmonotonic* with N and that the nonmonotonicity is caused by the dominant contribution of the intraband transition to γ_N in polyenes. Several important physical effects are discussed to reduce quantitative discrepancies between experimental and our results.

The size saturation behavior of the second-order hyperpolarizability $\gamma_N[-(\omega_1 + \omega_2 + \omega_3); \omega_1, \omega_2, \omega_3]$ of finite conjugated polymer (especially simple polyene chains) has been extensively studied both experimentally [1–5] and theoretically [6–21] for the past several decades. A power law on molecular size with variable power exponent is often used to describe the magnitude of the off-resonant nonlinear response in scaling. That is, $\gamma_N \sim N^b$, where N is the number of double bonds [2, 3]. The scaling is expected to saturate for the large N (thermodynamic limit), i.e., $b = 1$ as $N \rightarrow \infty$. Several measurements on cubic optical nonlinearity in long-chain polyene oligomers [2, 3] have shown the following three main features of the size dependence: (i) the exponent $b \sim 3 - 3.5$ for small N ; (ii) γ_N/N is *nonmonotonic* as a function of N , that is, γ_N/N increases with N initially, and after having reached a maximum value, then gradually decreases (about 10%) to the saturation value as N increases; (iii) the onset of the saturation occurs at $N \sim 90$ by the *nonmonotonic* fitting. We remark here that the nonmonotonicity of γ_N/N has been overlooked by most theoretical computations, and that in Ref. [3] the experimental data were fitted by a monotonic curve within experimental error and the onset of the saturation occurs at $N \sim 60$ by the *monotonic* fitting.

Theoretical studies range from simple tight-binding such as Hückel or Su-Schrieffer-Heeger (SSH) models [6–11] to Parier-Parr-Pople (PPP) [14, 15], Hubbard [16] and electron-hole pairs models [17, 18]. Detailed quantitative comparisons between experiments and theories are quite difficult due to the following several reasons. First, most theoretical studies have been limited to planar *trans*-polyenes, while the polyene chains in the solution are usually ‘disordered’

(*) Author to whom correspondence should be addressed. Email: mx200@nyu.edu

or ‘worm-like’ [3]. Second, experiments used series of polymers that, although related to polyenes, contain a central phenyle ring and incorporate rings that are saturated aside from a double bond in the “polyene” [3]. Third, the optical gaps are around 2.3 eV rather than typical polyacetylene’s 1.8 eV in most theoretical studies [3]. Hence, even under the same assumption of the planar structure of polyene chains, different models coupled with various (analytic and/or numeric) approximations have predicted vastly different γ_N and saturation behaviors for polyenes [6–21].

In this letter, based on the SSH model and our previous work [22, 23], we have derived an exact expression for the second-order hyperpolarizability of third-harmonic-generation (THG) $\gamma_N(-3\omega; \omega, \omega, \omega)$ for the finite chain of N double bonds. By choosing the typical parameters for polyenes, we notice that the exponent b varies from 2 to 5 for small N ($N < 21$) in our computation. Our result also shows strong nonmonotonicity of γ_N/N versus N . These match the experimental observations (i) and (ii) mentioned above. Finally, we observe that there are large quantitative discrepancies between this theoretical study and experiments in observation (iii) and the magnitude of γ_N/N .

Our computation shows that γ_N can be split into two parts: a positive part due to intraband transitions and a negative part due to interband transitions. The positive contribution from intraband transitions dominates the negative contribution from interband transitions. A positive γ_N in our computation is consistent with all existing polyene experiments [1–4] which show that γ_N is positive for any N . Moreover, we have carefully treated the so-called unphysical interference effects mentioned in the previous calculation [18]. Our results show that they can actually be identified as the boundary effects. Finally, since the zero-frequency limit $\gamma_N(0; 0, 0, 0)/N$ can not be measured directly, most experimentalists first measure the THG spectrum $\gamma_N(-3\omega; \omega, \omega, \omega)/N$ by choosing the frequency close to its three-photon resonance [2, 3] or the second-harmonic-generation spectrum $\gamma_N(-2\omega; \omega, \omega, 0)/N$ [4], then apply the empirical extrapolation to obtain $\gamma_N(0; 0, 0, 0)/N$. This empirical extrapolation largely depends on the three-photon-resonance of polyenes, but it also needs information on the linear absorption of solvent [2, 3]. Here we have derived the exact expressions for both the static hyperpolarizability ($\omega = 0$) and dynamic hyperpolarizability THG ($\omega \neq 0$). This could provide us some physical examinations of those empirical extrapolation methods. Despite the ignorance of Coulomb interactions [1, 12–18] and some other important effects (such as the effects of end groups [5], the conformational disorder [24], the solvent effect [25], the segments or short conjugation length [20, 21], etc) that must be considered in the more accurate quantitative calculations on one-dimensional(1D) polymers, our results show that the non-interacting SSH model (which is only first approximation of real physical systems) can nevertheless provide a clear understanding of the qualitative physical pictures of the saturation behavior.

The Hamiltonian for the SSH model [26] is given by:

$$H = - \sum_{l,s} [t_0 + (-1)^l 2\alpha u] (\hat{C}_{l+1,s}^\dagger \hat{C}_{l,s} + \hat{C}_{l,s}^\dagger \hat{C}_{l+1,s}) + 2nKu^2, \quad (1)$$

where t_0 is the transfer integral or hopping between the nearest-neighbor sites, u is the dimerization displacement, α is the changing rate of the hopping, n is the total number of CH monomers, K is the elastic constant, and $\hat{C}_{l,s}^\dagger$ ($\hat{C}_{l,s}$) creates(annihilates) an π electron at site l with spin s . Each site is occupied by one electron. With the lattice constant a and the definition of gap parameter $\Delta \equiv 4\alpha u$, we have the eigenenergies:

$$\varepsilon_v(k) = -\varepsilon_c(k) = -\sqrt{[2t_0 \cos(ka)]^2 + [\Delta \sin(ka)]^2}, \quad (2)$$

where $\varepsilon_v(k)$ and $\varepsilon_c(k)$ correspond to eigenenergies in the valence and conduction bands, re-

spectively. To avoid Jahn-Teller effects [14, 27], we work with the nondegenerate ground states of Hückel chain with $n = 4m + 2$ sites. Therefore, for a polyene chain with $N(\equiv n/2)$ double-bonds, the pseudo-momentum vector $\mathbf{k} = 0, \pm\pi/Na, \dots, \pm(2N-1)\pi/(4Na)$.

We resolve this size dependence problem via the following two steps. First, for each N we fix t_0 , α and K to find the minimum energy of the ground state in Eq. 1 by varying u . When the minimum energy is achieved, we denote the corresponding value of u by u_0 . Second, under the static lattice configuration determined by u_0 , we obtain an exact expression for γ_N for the dimerized Hückel chain with N double bonds. This two-step treatment takes into account the fact that π electrons make a much greater contribution to the γ_N in polyene chain than nuclei and σ electrons [1]. The Peierls instability in the quasi-1D polymer system [28] is also carefully considered in this method.

By choosing $t_0 = 2.5eV$, $\alpha = 4.1eV/\text{\AA}$, $K = 18.0eV/\text{\AA}^2$ and $a = 1.22\text{\AA}$, we obtain the energy gap $E_g \sim 1.89eV$ and $u_0 \sim 0.058\text{\AA}$ when $N \rightarrow \infty$. Both values are a little bit larger than those in the reported experiments where $u_0 \sim 0.04\text{\AA}$ and $E_g \sim 1.8eV$ [28]. However, the above parameters are not unreasonable since non-interacting models neglect the important Coulomb interactions in the 1D polymer chains [28]. The inclusion of the strong Coulomb interactions are generally expected to reduce the dimerized constant u_0 , hence it reduces the gap parameter Δ and the energy gap E_g [28] as well.

Table.I shows the relationship between N , u_0 , 2Δ and E_g . We would like to point out that there is no dimerization distortion for the extremely short chain with $N < 5$. A Peierls-type distortion toward a bond-alternated geometric structure with 14 or more π electrons has also been reported in the semiempirical calculations of cyanine dyes [1]. Since the dimerization distortion only exists for a reasonable size of polyene chains, we apply our calculation of γ_N only for $N \geq 5$.

Following the same procedures that have been developed in our previous work [22, 23] and by using the discrete summation of wave vectors \mathbf{k} instead of integrals, we obtain the following expression for the THG hyperpolarizability for a single finite chain:

$$\begin{aligned} \gamma_N(-3\omega; \omega, \omega, \omega) = & \frac{e^4 a^4}{512\delta^7 t_0^3} \sum_{k(\text{occ})} \left\{ \left[\frac{1}{2x^9(x^2 - z^2)} - \frac{9}{2x^9(x^2 - (3z)^2)} \right] \right. \\ & \left. - (1 - \delta^2 x^2)(x^2 - 1) \left[\frac{216}{x^9(x^2 - (3z)^2)} - \frac{252}{x^7(x^2 - (3z)^2)^2} - \frac{24}{x^9(x^2 - z^2)} - \frac{12}{x^7(x^2 - z^2)^2} \right] \right\}, \end{aligned} \quad (3)$$

where $\delta \equiv \Delta/2t_0$, $x \equiv \varepsilon_c(k)/\Delta$ and $z \equiv \hbar\omega/2\Delta$. Eq. 3/(2Na) recovers $\chi^{(3)}(-3\omega; \omega, \omega, \omega)$ for the infinite chain as $N \rightarrow \infty$ [23]. The first two terms in Eq. 3 correspond to the contributions from the interband transitions while the remaining terms correspond to those from the intraband transitions.

For the finite chain, the expressions of $\chi^{(3)}$ or γ_N/N also have another boundary term [29]. We have neglected this term in our study due to the following physical reasons. First, the boundary term disappears when $N \rightarrow \infty$. Second, it causes the so-called strong unphysical interference effects if it is included [18]. Third, the actual measurement of polyene materials in the solvent solution [2, 3] are on chain but not on ring structures, and the random phase on two open ending groups should be expected. Therefore, the boundary term should not have any observable effect or play a strong role in real physical environments.

The existing optical experiments are measured under the wavelength $\lambda = 1.91\mu\text{m}$ (or $\hbar\omega \sim 0.65eV$) [2, 3]. This wavelength is very close to the edge of three-photon resonance. In order to guarantee the THG transition in the off-resonant region, we have chosen $\hbar\omega = 0.6eV$ in our calculation. Substituting the parameters in Table. I into Eq. 3, we have computed

$\gamma_N(-3\omega; \omega, \omega, \omega)/N$ for $\hbar\omega \equiv 0.6eV$ and $\hbar\omega \equiv 0eV$. The results are shown in Fig.1A and in Fig.1B, respectively. On the same graphs, we have also compared them with the existing experimental results [3]. The graphs clearly show that the positive contribution from intraband transitions always dominates the negative contribution from interband transitions for any N . The fact that γ_N is positive in our calculation agrees with the reported experiments [1]. It is also consistent with the theory presented by Agrawal *et. al.* [6], but differs from McIntyre *et. al.*'s [7] and Beratan *et. al.*'s [8] results where only the negative interband contributions are considered.

Fig.1 shows γ_N/N firstly increases until N reaches about 20-30 and then decreases thereafter. Though this trend is parallel to the *nonmonotonic* feature in existing experiments [2,3], it has never been reported in the existing theories [6-21]. γ_N/N curve has a much longer tail and almost 2 orders larger value for $\hbar\omega = 0.6eV$ than its static limit $\hbar\omega = 0.0eV$. It shows that the three-photon resonance plays a strong role to saturate at a relatively large N . $\gamma_N(-3\omega; \omega, \omega, \omega)/N$ saturates at $N_{sat}^\gamma \sim 60$ for $\hbar\omega = 0.6eV$ while at $N_{sat}^\gamma \sim 40$ for its static counterpart. The much larger saturation length and γ_N value at finite frequencies than at the static limit has also been reported in Luo *et. al.*'s work [30]. Our calculated N_{sat}^γ mismatches worse at $0eV$ than at $0.6eV$ with the experiments that report $N_{sat}^\gamma \sim 60$ (without considering *slight nonmonocity*) for both cases [2,3]. The N_{sat}^γ difference between this calculation and experiment for $0eV$ could be understood because the experiment uses the following extrapolation formula to obtain the static limit [2,3]:

$$\gamma_N(0; 0, 0, 0) = \frac{1 - (\lambda_{max}/\lambda)^2}{1 - (3\lambda_{max}/\lambda)^2} \gamma_N(-3\omega; \omega, \omega, \omega), \quad (4)$$

where λ_{max} and λ correspond to the wavelength of the maximum of the absorption in solution and the measurement, respectively. Eq. 4 assumes that $\gamma_N(0; 0, 0, 0)$ is largely dependent on the three-photon process in $\gamma_N(-3\omega; \omega, \omega, \omega)$. However, Eq. 3 shows that the one-photon process ($(x^2 - z^2)^{-1}$ terms) in γ_N plays a much more important role at its static limit, even if it is very small compared to its three-photon counterpart at $\hbar\omega = 0.6eV$. The one-photon's contribution was ignored in the above experimental extrapolation formula.

The one-photon's influence on the saturation behavior in γ_N/N is similar to that of linear susceptibility $\chi_N^{(1)}$. Fig.2 is plotted according to Eq.(3.13) in Ref. [22]. $\chi_N^{(1)}$ saturates at $N_{sat}^\alpha \sim 25 \pm 2$. The *non-monotonic* γ_N/N up-and-down trend is dominated by the intraband contributions and are closely related with the linear saturation N_{sat}^α . The intraband contributions are determined by gradient \mathbf{k} terms or \mathbf{k} -changing rate of dipole-transitions [6, 23]. The intraband γ_N^{intra} drastically increases with N until N reaches N_{sat}^α , then the increasing of N (corresponding to the additional π -electron) lowers the average contribution of γ_N^{intra} until γ_N^{intra}/N reaches its static limit. Meanwhile the negative but relatively weak interband γ_N^{inter} increases monotonically with N to its static limit. This may explain the up-and-down features of γ_N/N in experiments [2,3].

Our theoretical results of $N_{sat}^\gamma \sim 40$ and $N_{sat}^\alpha \sim 25$ at $\omega = 0$ are in agreement with Lu *et. al.*'s ab initio calculations of polyene ($N_{sat}^\gamma = 45 \pm 5$ and $N_{sat}^\alpha = 25 \pm 2$) [19]. They are also comparable with the work of Shuai and Brédas ($N_{sat}^\gamma \sim 50$) [9], Yu and Su ($N_{sat}^\gamma \sim 50$) [10] and Spano and Soos ($N_{sat}^\gamma \sim 30$ for $\delta \approx 0.18$) [11]. We have applied a factor of 1/2 on the number of n -site carbon to convert the results in Ref. [9-11].

Fig.3 shows the scaling power b versus N . b varies with both N and ω . It is also very sensitive to some other factors such as the hopping t_0 , gap parameter Δ , etc [9-11]. The scaling power law has also been extensively studied in many theoretical works [8-19]. Due to the fact that b is a derivative from γ_N , here we only make a simple discussion. For $N=9$, we

have $b = 4.83$ at $0.6eV$ and $b = 2.91$ at the static limit. The steadily decreasing trend in the graph is quite similar to Fig.4 ($\delta = 0.18$) in Ref. [11] when $N \leq 30$.

Some quantitative discrepancies between this calculation and the existing experiments [2,3] are evident. Although a much large or upper bound limit of γ_N value should be expected under the Hückel model due to the ignorance of Coulomb interactions [11,14], theoretical values of γ_N/N are much larger than experimental data especially when $\hbar\omega = 0.6eV$. There are many factors to influence this result. One chief factor could be the conformational behavior in the solvents [3,24,25] and the fact that the polyene chain is no longer oriented in one direction. Hence the worm-like polymer chains may significantly reduce γ_N value by averaging the contribution in 3D space. The segment or short conjugation length treatment of polyene chains may also reduce γ_N [20,21]. Another important factor is the damping or the lifetime of excited states [9]. This may smear off the resonant peak and hence reduce γ_N . The optical gap Δ of experimental “polyene” is around $2.3 eV$ while ours is $1.9 eV$. Since $\gamma_N/N \sim \Delta^{-6}$ [6], theoretical values would be about $(2.3/1.9)^6 \approx 3.2$ times as large as the experimental data due to this factor alone. Finally, the nondegenerate ground state resulting from the end groups or fixed ring structures [3–5] in experiments may also play a role.

In conclusion, the study of the size dependence of γ_N based on the SSH model provides us a solid physical background to understand the saturation behaviors in polyene systems. Most valuable features of in the experiments of γ_N could be qualitatively explained under the schema of single-electron models. However, the quantitative comparison with the existing experiments in 1D polymer system still shows that the SSH model is only first approximation for real physical systems. Further studies require the refinement of the model with the consideration of many other important factors such as the Coulomb interactions, conformational behaviors, segments effects of chains, solvent effects or the damping factor, etc.

REFERENCES

- [1] Brédas J. L., Adant C., Tackx P., Persoons A., and Pierce B. M., *Chem. Rev.* **94**, 243 (1994).
- [2] Samuel I. D. W., Ledoux I., Dhenaut C., Zyss J., Fox H. H., Schrock R. R., and Silbey R. J., *Science* **265**, 1070 (1994).
- [3] Ledoux I., Samuel I. D. W., Zyss J., Yaliraki S. N., Schattenmann F. J., Schrock R. R., and Silbey R. J., *Chem. Phys.* **245**, 1 (1999).
- [4] Craig G. S. W., Cohen R. E., Schrock R. R., Silbey R. J., Puccetti G., Ledoux I., and Zyss J., *J. Am. Chem. Soc.* **115**, 860 (1993).
- [5] Puccetti G., Blanchard-Desce M., Ledoux I., Lehn J-M., and Zyss J., *J. Phys. Chem.* **97**, 9385 (1993).
- [6] Agrawal G. P., Cojan C., and Flytzanis C., *Phys. Rev. B* **17**, 776 (1978).
- [7] McIntyre E. F. and Hamerka H. F., *J. Chem. Phys.* **68**, 3481 (1978).
- [8] Beratan D. N., Onuchic J. N., and Perry J. W., *J. Phys. Chem.* **91**, 2696 (1987).
- [9] Shuai Z. and Brédas J. L., *Phys. Rev. B* **44**, R5962 (1991).
- [10] Yu J. and Su W. P., *Phys. Rev. B* **44**, 13315 (1991).
- [11] Spano F. C. and Soos Z. G., *J. Chem. Phys.* **99**, 9265 (1993).
- [12] DeMelo C. P. and Silbey R. J., *J. Chem. Phys.* **88**, 2587 (1987).
- [13] Heflin J. R., Wong K. Y., Zamani-khamiri O., and Garito A. F., *Phys. Rev. B* **38**, 1573 (1988).
- [14] Soos Z. G. and Ramasesha S., *J. Chem. Phys.* **90**, 1067 (1989).
- [15] Yaron D. and Silbey R. J., *Phys. Rev. B* **45**, 11655 (1992).
- [16] Zhang G. P., *Phys. Rev. B* **60**, 11482 (1999).
- [17] Mukamel S., Takahashi A., Wang H. X. and Chen G., *Science* **266**, 250 (1994).
- [18] Toury T., Zyss J., Chernyak V., and Mukamel S., *J. Phys. Chem. A* **105**, 5692 (2001).

- [19] Lu D., Marten B., Ringnalda M., Friesner R. A., and Goddard III W. A., *Chem. Phys. Lett.* **257**, 224 (1996).
- [20] Kohler B. E. and Samuel I. D. W., *J. Chem. Phys.* **103**, 6248 (1995).
- [21] Kohler B. E. and Woehl J. C., *J. Chem. Phys.* **103**, 6253 (1995).
- [22] Xu M. Z. and Sun X., *J. Phys. Condens. Matter* **11**, 9823 (1999).
- [23] Jiang S. D. and Xu M. Z., *J. Chem. Phys.* **123**, 064901 (2005).
- [24] Rossi G., Chance R. R., and Silbey R. J., *J. Chem. Phys.* **90**, 7594 (1989).
- [25] Luo Y., Norman P., Macak P., and Agren H., *J. Chem. Phys.* **111**, 9853 (1999).
- [26] Su W. P., Schrieffer J. R., and Heeger A. J., *Phys. Rev. Lett.* **42**, 1698 (1979).
- [27] Kivelson S., Lee T. K., Lin-Liu Y. R., Peschel I., and Yu L., *Phys. Rev. B* **25**, 4173 (1982).
- [28] Heeger A. J., Kivelson S., Schrieffer J. R., and Su W. P., *Rev. Mod. Phys.* **60**, 781 (1988).
- [29] Jiang S. D. and Xu M. Z., 'Hyperpolarizabilities for the one-dimensional infinite single-electron periodic systems: III. Size scaling law under the dimerized Hückel model', in preparations.
- [30] Luo Y., Ruud K., Norman P., Jonsson D., and Ågren H., *J. Phys. Chem. B* **102**, 1710 (1998).

TABLE I – *Relationship between number of double bonds N , dimerized constant u_0 , gap parameter 2Δ and actual energy gap E_g . ($t_0 = 2.5eV$, $\alpha = 4.1eV/\text{\AA}$ and $K = 18.0eV/\text{\AA}^2$).*

| N | $u_0(\text{\AA})$ | $2\Delta(eV)$ | $E_g(eV)$ |
|-----|-------------------|---------------|-----------|
| 5 | 0.0073 | 0.238 | 3.098 |
| 7 | 0.0481 | 1.576 | 2.704 |
| 9 | 0.0542 | 1.779 | 2.467 |
| 11 | 0.0562 | 1.843 | 2.314 |
| 13 | 0.0569 | 1.868 | 2.211 |
| 15 | 0.0572 | 1.877 | 2.140 |
| 17 | 0.0574 | 1.882 | 2.088 |
| 19 | 0.0574 | 1.883 | 2.051 |
| 21 | 0.0574 | 1.884 | 2.022 |
| 23 | 0.0575 | 1.885 | 2.000 |
| 41 | 0.0575 | 1.885 | 1.922 |
| 81 | 0.0575 | 1.885 | 1.894 |
| 251 | 0.0575 | 1.885 | 1.886 |

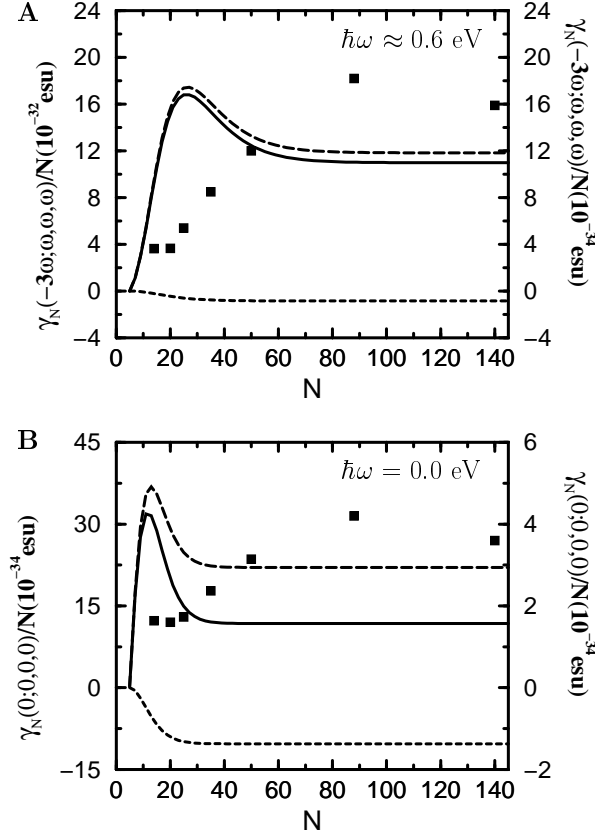


Fig. 1 – **A.** Computed THG $\gamma_N(-3\omega; \omega, \omega, \omega)/N$ at $\hbar\omega = 0.6$ eV (left Y scale in units of 10^{-32} esu): total contribution (solid line), intraband contribution (long dashed line) and interband contribution (short dashed line) versus the experimental THG result $\gamma_N(3\omega)/N$ (Ref.3) at $\lambda = 1.91\mu\text{m}$ (solid square and the right Y scale in units of 10^{-34} esu); **B.** Computed static $\gamma_N(0; 0, 0, 0)/N$ (left Y scale in units of 10^{-34} esu): total contribution (solid line), intraband contribution (long dashed line) and interband contribution (short dashed line) versus the experimental extrapolation static $\gamma_N(0)/N$ (Ref.3) (solid square and right Y scale in units of 10^{-34} esu).

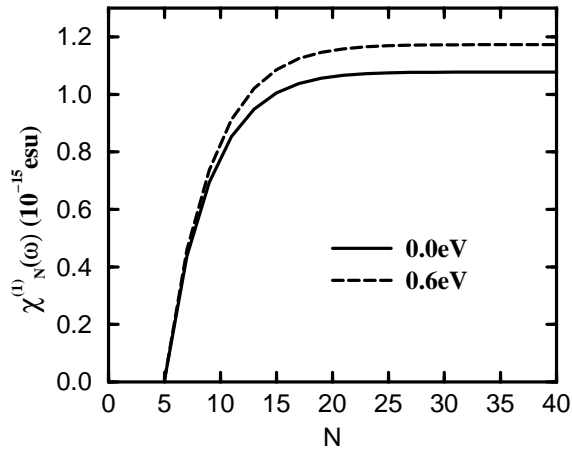


Fig. 2 – Computed linear susceptibility $\chi^{(1)}(N, \omega)$ versus N at $\hbar\omega = 0.0eV$ and $\hbar\omega = 0.6eV$ for $N \geq 5$.

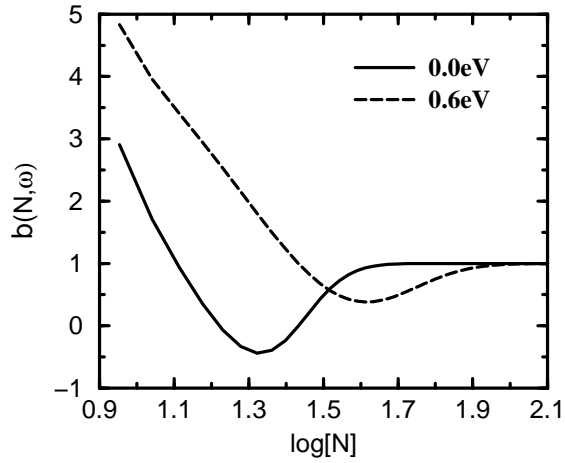


Fig. 3 – Computed scaling power coefficient $b(N, \omega) \equiv d[\log\gamma_N(-3\omega; \omega, \omega, \omega)]/d[\log N]$ versus $\log N$ at $\hbar\omega = 0.0eV$ (solid line) and $\hbar\omega = 0.6eV$ (long dashed line) for $N \geq 9$.